Charge/Orbital Ordering Structure of $Pr_{1-x}Ca_xMnO_3$ ($x = 3/8$) Examined by Low-Temperature Transmission Electron Microscopy

T. Asaka,[1,2] S. Yamada,[3] S. Tsutsumi,[2] C. Tsuruta,[1] K. Kimoto,[1] T. Arima,[3] and Y. Matsui[1]

[1]*Advanced Materials Laboratory, National Institute for Materials Science, Tsukuba 305-0044, Japan*

[2]*School of Education, Waseda University, Tokyo, 169-8085 Japan*

[3]*Institute of Materials Science, University of Tsukuba, Tsukuba 305-8573, Japan*

(Received 23 July 2001; published 14 February 2002)

The structural phase transition of $Pr_{1-x}Ca_xMnO_3$ ($x = 3/8$) was investigated by means of low-temperature transmission electron microscopy. Superlattice reflection spots with a modulation wave vector $\boldsymbol{q}_1 = (0, 1/2, 0)$ appeared below 230 K, indicating formation of the $d_{3x^2-r^2}/d_{3y^2-r^2}$ type of charge/orbital ordering. Below 150 K, a new series of superlattice reflection spots with a modulation wave vector $\boldsymbol{q}_2 = (1/4, 1/4, 1/2)$ appeared, suggesting an additional ordering of excess 1/8 Mn^{3+}, necessary due to the deviation of x from 1/2, with the occupation of the $d_{3z^2-r^2}$ type of e_g orbital.

DOI: 10.1103/PhysRevLett.88.097201 PACS numbers: 75.30.Vn, 64.70.Kb, 71.27.+a, 71.30.+h

Perovskite-type manganese oxides with the general formula $RE_{1-x}AE_xMnO_3$ (*RE* and *AE* being rare- and alkaline-earth ions, respectively) have attracted considerable attention because of their unusual electrical and magnetic properties. Some of these properties are associated with a charge-ordering state in which Mn^{3+} and Mn^{4+} are arranged alternatively. This charge ordering occurs in manganese oxides with a small one-electron bandwidth [1–8]. In $Pr_{1-x}Ca_xMnO_3$, the charge-ordering phase has been observed for a wide range of x ($0.3 \leq x \leq 0.75$) [9,10]. It has been reported that the charge ordering in the system can be melted by the application of magnetic [11,12] or electric fields [13], or by x-ray [14], visible-IR light [15], or electron [16] irradiation. Based on the x dependence of the magnetic field necessary to melt the charge ordering for $x < 1/2$ compounds, Tomioka *et al.* reported that deviation of x from 1/2 changes the robustness of the charge-ordering state [11]. The charge ordering is accompanied by an ordering of e_g orbitals of the $d_{3x^2-r^2}/d_{3y^2-r^2}$ type and the cooperative Jahn-Teller distortion [2–4,17]. Here, the x, y, and z axes were nearly parallel to [110], $[\bar{1}10]$, and [001], respectively, in the *P*bnm orthorhombically distorted perovskite. Superlattice reflections found in the diffraction patterns were evidence of orbital ordering.

The modulation wave vector of superlattice reflection for compounds with $x \geq 1/2$ corresponds to the hole-doping level. For example, the modulation wave vectors for compounds with $x = 1/2$ and 2/3 are $(0, 1/2, 0)$ [3,4,10] and $(0, 1/3, 0)$ [5,6,8], respectively. In contrast, the $(0, 1/2, 0)$ superlattice reflection is always observed for $Pr_{1-x}Ca_xMnO_3$ with $0.3 \leq x \leq 0.5$ [10,18], which indicates orbital ordering with the same periodicity as $x = 1/2$. Jirak *et al.* [10] interpreted this phenomenon as demonstrating that an e_g orbital with an occupancy of less than one existed on the Mn^{4+} sites based on the results from their powder neutron diffraction experiments. Concerning the charge ordering of $Pr_{1-x}Ca_xMnO_3$ with $x \leq 0.5$, Okimoto *et al.* [19] have demonstrated that a charge gap exists in the optical absorption for the polarization along the c axis of $Pr_{1-x}Ca_xMnO_3$ ($x = 0.4$). More recently, Yamada *et al.* [20] stated, based on their thermopower study, that spatial ordering of extra e_g electrons should occur when $x \sim 0.35$.

In this paper, we report on our low-temperature electron diffraction and electron microscopy studies of $Pr_{1-x}Ca_xMnO_3$ ($x = 0.375$, i.e., 3/8). Our analysis of the electron diffraction patterns has revealed a new form of structural modulation, and we discuss its origin in terms of the ordering of extra e_g electrons. This is the first experimental evidence of spatial ordering of extra e_g electrons as far as we know.

We grew single crystalline samples of $Pr_{0.625}Ca_{0.375}MnO_3$ by a floating-zone method. (The crystal growth details have been given elsewhere [21].) We used two procedures to prepare the electron diffraction and electron microscopy specimens. Some samples were ground under CCl_4 then dispersed on Cu grids coated with holy-carbon support films, and the others were thinned by Ar^+ ion sputtering. The specimens were examined with a Hitachi H-1500 high-voltage transmission electron microscopy (TEM) operating at 800 kV, and with Hitachi HF-3000S and HF-3000L field-emission TEMs operating at 300 kV.

The electron diffraction patterns obtained from $Pr_{5/8}Ca_{3/8}MnO_3$ at room temperature indicate a *P*bnm orthorhombic structure with lattice parameters $a \approx b \approx \sqrt{2}\,a_P$ and $c \approx 2a_P$ (a_P: the lattice constant of the simple cubic perovskite cell). The typical [001]-zone electron-diffraction pattern at room temperature is shown in Fig. 1(a). Here, the $h00$, $0k0$, and $00l$ reflections with h, k, and $l = 2n + 1$ (n: integer), respectively, are caused by double diffraction.

We focus here on our low-temperature investigation of the charge-ordering transition in $Pr_{5/8}Ca_{3/8}MnO_3$. We cooled the samples from room temperature and observed traces of diffuse scattering that were slightly extended in

 © 2002 The American Physical Society

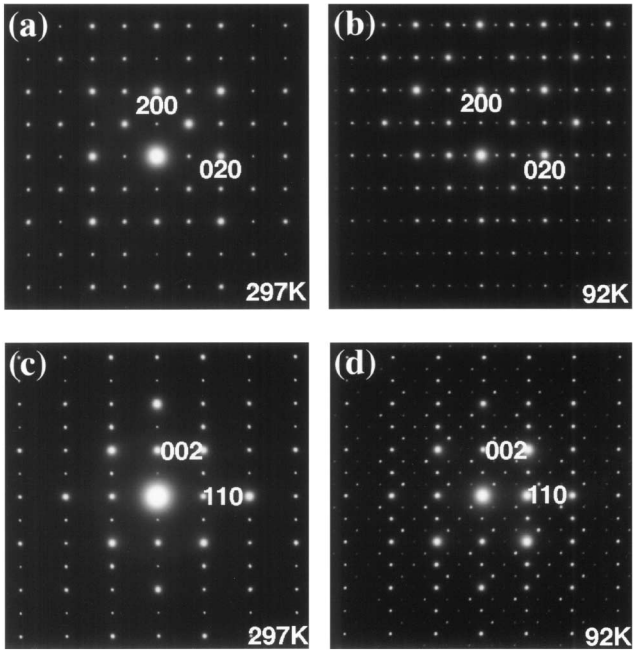

FIG. 1. [001]-zone electron-diffraction patterns of $Pr_{5/8}Ca_{3/8}MnO_3$ obtained at (a) room temperature and (b) 92 K, respectively. The presence of superlattice reflections with a modulation wave vector $(0, 1/2, 0)$ is evident. $[\bar{1}10]$-zone electron-diffraction patterns obtained at (c) room temperature and (d) 92 K, respectively. The presence of superlattice reflections along the [112] direction is evident. The wave vector of these superlattice reflections is shown as $\boldsymbol{q}_2$ in the text. Note the possibility that twin domains of $\boldsymbol{q}_2$ modulation are shown in (d).

the b^* direction below 260 K, and then became superlattice reflection spots below 230 K. Figure 1(b) shows the [001]-zone electron-diffraction pattern at 92 K. As compared with the pattern at room temperature, additional superlattice reflections with a modulation wave vector $\boldsymbol{q}_1 = (0, 1/2, 0)$ appeared. We performed the same electron diffraction experiments on $Pr_{1-x}Ca_xMnO_3$ with $x = 0.3$, 0.35, 0.4, 0.45, and 0.5, and all samples had the same superstructure with $\boldsymbol{q}_1$ at 92 K. This feature is in stark contrast to the above mentioned case of $x \geq 1/2$. Furthermore, the temperature dependence of the $\boldsymbol{q}_1$ superlattice reflections for the $x < 1/2$ compounds differed from that for the $x \geq 1/2$ compounds. While incommensurate superlattice reflections were observed for the compounds with $x \geq 1/2$ above the antiferromagnetic spin-ordering temperature T_N [3,4,7,22], the superlattice reflections for the present compounds with $x < 1/2$ were always observed at the commensurate positions and only changed in intensity at $T_N < T < T_{CO}$. The $\boldsymbol{q}_1$ superstructure reflections in the $x = 1/2$ compounds are ascribed to the $d_{3x^2-r^2}/d_{3y^2-r^2}$ type of orbital ordering. The same type of charge/orbital ordering occurs in $Pr_{5/8}Ca_{3/8}MnO_3$ at low temperatures.

At lower temperatures, superstructure reflections with another modulation wave vector from $\boldsymbol{q}_1$ were found. Figure 1(d) shows the $[\bar{1}10]$-zone electron-diffraction pattern of $Pr_{5/8}Ca_{3/8}MnO_3$ at 92 K. Sharp superstructure reflections, which were not observed at room temperature [Fig. 1(c)], can be seen. The modulation wave vector is commensurate and can be denoted as $\boldsymbol{q}_2 = (1/4, 1/4, 1/2)$. The superstructure reflections with $\boldsymbol{q}_2$ appear as very weak diffuse scattering below 150 K. As the temperature decreased, the intensities of the superlattice reflections increased. However, while the diffuse scattering became superlattice spots below 100 K, the wave vector $\boldsymbol{q}_2$ did not charge throughout the cooling. Upon warming from 92 K, the $\boldsymbol{q}_2$ superlattice reflections remained as diffraction spots with decreasing intensity up to 200 K. They subsequently became diffuse scattering, and then completely disappeared at about 250 K. The temperature dependence of the $\boldsymbol{q}_1$ superlattice reflections was qualitatively the same as the behavior of the $\boldsymbol{q}_2$ superlattice reflections described above. The $\boldsymbol{q}_1$ superlattice reflections changed into diffuse scattering at about 200 K and disappeared at about 270 K. The intensities of both the $\boldsymbol{q}_1$ and $\boldsymbol{q}_2$ superlattice reflections show large hystereses between cooling and warming.

Here we discuss the origin of the $\boldsymbol{q}_2$ reflections. As shown in Fig. 1(d), the intensities of the first-order superlattice reflections near fundamental spots are higher than for second-order ones. This indicates that the fundamental structure is modulated by periodic shifts in atomic position. The $\boldsymbol{q}_2$ superlattice reflections should not be ascribed to a twin structure of two domains in the direction of the [001] and $[\bar{1}10]$ zone axis, taking account of the features in the electron-diffraction pattern and the subsequent lattice image. The $[\bar{1}10]$-zone lattice image shown in Fig. 2

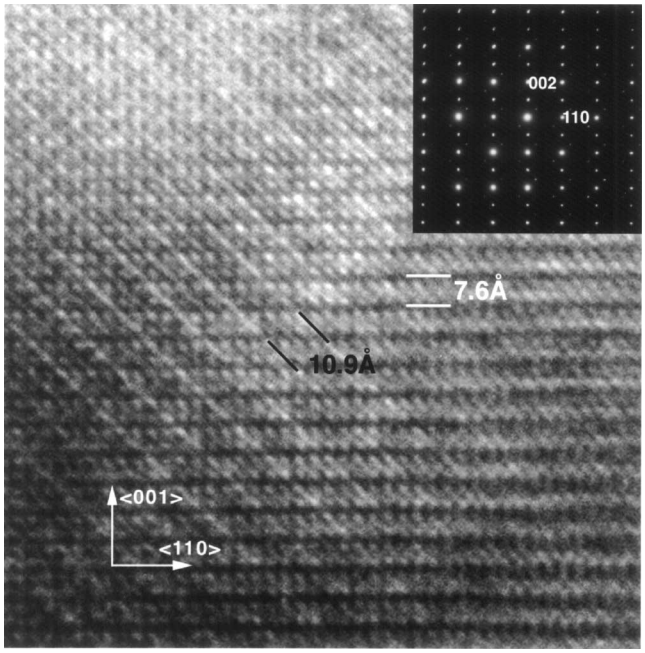

FIG. 2. $[\bar{1}10]$-zone lattice image obtained at 80 K. In addition to the contrast of the lattice constant c (~7.6 Å), the contrast of the $\boldsymbol{q}_2$ superlattice is shown obliquely. The inset is the corresponding electron diffraction pattern.

undoubtedly indicates that this material has a modulation structure at 80 K. The 7.6-Å periodic contrasts, corresponding to the lattice constant c, are overlaid obliquely with the 10.9-Å modulation contrasts, corresponding to the magnitude of $\boldsymbol{q}_2$. Furthermore, the $\boldsymbol{q}_1$ and $\boldsymbol{q}_2$ superlattice spots began to appear at different temperatures, as mentioned above. Therefore, the $\boldsymbol{q}_2$ modulation structure does not originate from twin domains.

We prove in the following that the $\boldsymbol{q}_1$ and $\boldsymbol{q}_2$ modulation structures exist in the single domain and are not caused by any other phases that result from phase separation or imhomogeneity of the chemical composition. Figure 3(a) shows the dark field image formed by a $\boldsymbol{q}_2$ superlattice spot at 80 K. The bright parts are domains with the $\boldsymbol{q}_2$ modulation structure and the dark lines show antiphase boundaries. Rotating the specimen around the c axis by 45° causes the [100] (or [010]) zone-axis pattern shown in the inset of Fig. 3(b) to appear in the same part of the crystal. In this diffraction pattern, superstructure spots caused by the $\boldsymbol{q}_1$ modulation appeared. The dark field image formed by these spots is shown in Fig. 3(b). The bright parts caused by the $\boldsymbol{q}_1$ modulation structure approximately coincided with the $\boldsymbol{q}_2$ modulated domain shown in Fig. 3(a). [Note that the lines on the left in Fig. 3(b) show the twin boundaries. These boundaries did not appear in Fig. 3(a) because the crystal orientation is undesirable for the observation of this type of twin boundary, which is the twin boundary between the ac and the bc domains.] Therefore, this compound had $\boldsymbol{q}_1$ and $\boldsymbol{q}_2$ modulation structures in the same spatial distribution. Furthermore, when we examined the temperature dependence of the [100]-zone electron-diffraction pattern during the cooling stage, we observed a typical change in the $\boldsymbol{q}_1$ superlattice reflection spots. The electron diffraction patterns in the cooling stage at 297, 110, and 92 K are shown in Figs. 3(c), 3(d), and 3(e), respectively. Only the second-order reflections of the $\boldsymbol{q}_1$ modulation structure are discernible down to 110 K. We inferred from our analysis of the diffraction patterns that the space group is $P2_1/\mathrm{m}$. All the expected superlattice reflection spots caused by the $\boldsymbol{q}_1$ modulation structure appear at 92 K. This indicates that the symmetry probably becomes lower when both $\boldsymbol{q}_2$ and $\boldsymbol{q}_1$ modulation structures are formed simultaneously.

We interpret the cause of the $\boldsymbol{q}_2$ modulation structure in terms of the ordering of extra e_g electrons along the c axis. Here, we propose a possible model of a structure in charge/orbital ordered state for $Pr_{5/8}Ca_{3/8}MnO_3$. First, the $\boldsymbol{q}_1$ modulation structure, which is similar to the charge/orbital ordering in $La_{1/2}Ca_{1/2}MnO_3$ and $Pr_{1/2}Ca_{1/2}MnO_3$, must remain essentially. Second, Mn^{3+} ions must be substituted partially on the Mn^{4+} sublattice in the $x = 1/2$-type of charge ordering. In our model, charge ordering on this sublattice is very important. From the chemical composition, the ratio of Mn^{3+} to Mn^{4+} in this sublattice should be 1:3. The extra e_g electrons occupy $3d_{3z^2-r^2}$ orbitals on the Mn^{4+} sublattice, as in the model by

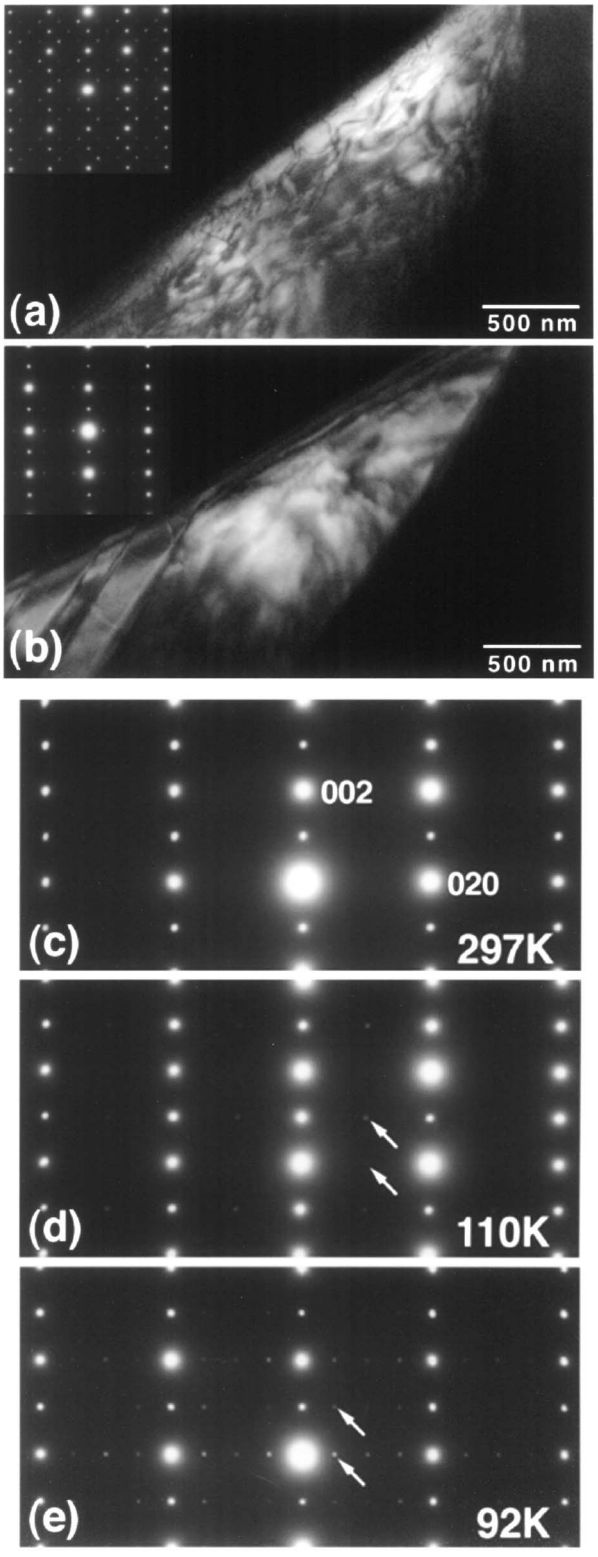

FIG. 3. Dark field images obtained from the superlattice reflections. (a) $[\bar{1}10]$ and (b) [100] zone-axis images from the same part of the crystal. The insets are the corresponding electron diffraction patterns. The image shown in (b) was obtained after 45° rotation of the sample around the c axis. The [100]-zone electron-diffraction patterns were obtained at (c) room temperature, (d) 110 K, and (e) 92 K. Arrows correspond to superlattice reflections with a modulation wave vector $\boldsymbol{q}_1$.

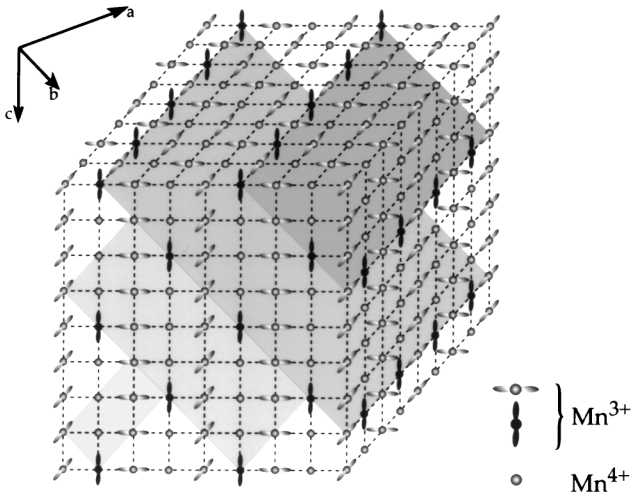

FIG. 4. Proposed model of the charge-orbital ordering structure for $Pr_{5/8}Ca_{3/8}MnO_3$. In this illustration, all ions except Mn are omitted.

Jirak *et al.* [10]. $Mn^{3+}O_6$ octahedra would accompany the Jahn-Teller distortion. Taking the direction of the $\boldsymbol{q}_2$ vector into consideration also, the proposed model is as shown in Fig. 4. The extra e_g electrons are shown as dark gray symbols of Mn^{3+} in the shadowed areas of Fig. 4. This model is consistent with the findings of previous optical [19] and thermopower [20] studies. A computer simulation based on this model also agrees fairly well with the obtained patterns.

In our model, the temperature dependence of the nucleation and growth of the $\boldsymbol{q}_2$ modulation structure can be interpreted as follows. During the first stage of cooling, it is conceivable that nucleation of the $\boldsymbol{q}_1$ superstructure occurs as short-range ordering that includes disordered planes with random occupation of e_g orbitals, perpendicular to the b axis, judging from the trace of diffuse scattering extent in the b^* direction in the [001]-zone diffraction patterns. If the orbital disordering planes are laid in the $\boldsymbol{q}_1$ orbital ordered phase, the $\boldsymbol{q}_2$ modulation structure will not be formed. The extra e_g electrons occupy the $d_{3z^2-r^2}$ orbital in the long-range orbital ordered state, as described above. In the short-range orbital ordering state, however, there is a possibility that the orbital disordering planes cause random occupation of extra e_g orbitals. Therefore, long-range orbital ordering of the $\boldsymbol{q}_1$ superstructure is necessary for nucleation and growth of the $\boldsymbol{q}_2$ modulation structure. In fact, when long-range orbital ordering of $\boldsymbol{q}_1$ was observed in the electron diffraction patterns and the dark field images of the $\boldsymbol{q}_1$ superstructure spots at lower temperatures, the $\boldsymbol{q}_2$ modulation structure was identified. This model also explains the lower $\boldsymbol{q}_2$ transition temperature. Moreover, it is worth mentioning that the onset temperature of the $\boldsymbol{q}_2$ modulation structure is close to the antiferromagnetic spin-ordering temperature T_N, ~160 K [20].

In summary, we have investigated the crystal structure of $Pr_{5/8}Ca_{5/8}MnO_3$ in the charge/orbital ordering state by means of low-temperature TEM. Superlattice reflection spots with a modulation wave vector $\boldsymbol{q}_1 = (0, 1/2, 0)$ appeared below 230 K. With a further decrease in temperature, an additional modulation structure was generated. This modulation structure first appeared as diffuse scattering below 150 K, and then as sharp spots with a modulation wave vector $\boldsymbol{q}_2 = (1/4, 1/4, 1/2)$ below 100 K. We interpreted this modulation structure in terms of the charge/orbital ordering of extra Mn^{3+} ions. We also examined compounds with $x = 0.3$ to 0.5, and confirmed the appearances of $\boldsymbol{q}_2$ superstructure spots in the compounds with $x = 0.36$ to 0.4.

We are grateful to Professor Y. Tokura (University of Tokyo & JRCAT), Dr. Y. Tomioka (JRCAT), and Dr. Y. Okimoto (JRCAT) for their valuable discussions. We also thank Dr. M. Uchida, Y. Shiraishi, Y. Anan, and T. Nagai (AML.NIMS) for their collaboration and valuable discussions. Finally, we thank Dr. Z. Jirak (ASCR) for his fruitful comments and discussion.

[1] E. O. Wollan and W. C. Koehler, Phys. Rev. **100**, 545 (1955).
[2] J. B. Goodenough, Phys. Rev. **100**, 564 (1955).
[3] C. H. Chen and S-W. Cheong, Phys. Rev. Lett. **76**, 4042 (1996).
[4] P. G. Radaelli *et al.,* Phys. Rev. B **55**, 3015 (1997).
[5] C. H. Chen, S-W. Cheong, and H. Y. Hwang, J. Appl. Phys. **81**, 4326 (1997).
[6] A. P. Ramirez *et al.,* Phys. Rev. Lett. **76**, 3188 (1996).
[7] S. Mori, C. H. Chen, and S-W. Cheong, Nature (London) **392**, 473 (1998).
[8] M. T. Fernandez-Diaz *et al.,* Phys. Rev. B **59**, 1277 (1999).
[9] E. Pollert, S. Krupicka, and E. Kuzmicova, J. Phys. Chem. Solids **43**, 1137 (1982).
[10] Z. Jirak *et al.,* J. Magn. Magn. Mater. **53**, 153 (1985).
[11] Y. Tomioka *et al.,* J. Phys. Soc. Jpn. **64**, 3626 (1995); Y. Tomioka *et al.,* Phys. Rev. B **53**, R1689 (1996).
[12] H. Yoshizawa *et al.,* Phys. Rev. B **52**, R13 145 (1995).
[13] A. Asamitsu *et al.,* Nature (London) **388**, 50 (1997).
[14] V. Kiryakhin *et al.,* Nature (London) **386**, 813 (1997).
[15] K. Miyano *et al.,* Phys. Rev. Lett. **78**, 4257 (1997); M. Fiebig *et al.,* Appl. Phys. Lett. **74**, 2310 (1999); K. Ogawa *et al.,* Phys. Rev. B **57**, R15 033 (1998).
[16] M. Hervieu *et al.,* Phys. Rev. B **60**, 726 (1999).
[17] H. Kawano *et al.,* Phys. Rev. Lett. **78**, 4253 (1997); K. Nakamura *et al.,* Phys. Rev. B **60**, 2425 (1997); M. v. Zimmerman *et al.,* Phys. Rev. Lett. **83**, 4872 (1999).
[18] D. E. Cox *et al.,* Phys. Rev. B **57**, 3305 (1998).
[19] Y. Okimoto *et al.,* Phys. Rev. B **59**, 7401 (1999).
[20] S. Yamada *et al.,* J. Phys. Soc. Jpn. **69**, 1278 (2000).
[21] S. Yamada, T. Arima, and K. Takita, J. Phys. Soc. Jpn. **68**, 3701 (1999).
[22] S. Mori, C. H. Chen, and S-W. Cheong, Phys. Rev. Lett. **81**, 3972 (1998).